JOURNAL OF MATERIALS SCIENCE 16 (1981) 1925–1934

The fracture of highly crosslinked polymers

Part 2 *Fractography*

B. W. CHERRY, K. W. THOMSON
Department of Materials Engineering, Monash University, Clayton, Victoria, 3168 Australia

The fracture behaviour of five epoxy resin systems was investigated in a previous paper. The fracture surfaces formed over a wide range of testing rates have been examined. The fracture surface features correlate with the testing rate and indicate that slow stable propagation commonly precedes unstable fracture. A qualitative explanation for the transitions in fracture behaviour in terms of the effect of strain rate on yielding is presented.

1. Introduction

In a previous paper [1] five epoxy resin systems were characterized and their fracture behaviour over a wide range of testing rates was reported. Crack growth was found to proceed either by slow stable (type I) propagation, which may remain stable for several centimeters of crack growth (type IA) or become unstable after more limited extension (type IB); by fast unstable (type II) or fast stable propagation (type III). These classifications were based on the shape of the load–load-point displacement curves together with direct observation of the crack tip for slow crack growth.

Since a change in the fracture surface energy is likely to be reflected by a change in the topography of the fracture surface, fractography can make a major contribution towards the understanding of fracture instability. In particular, the present study was aimed at correlating the fracture behaviour with the fracture surface features in order to investigate the mechanisms of fracture.

2. Experimental procedure

Details of the epoxy systems and curing schedules have been given previously [1]. For the D/TETA specimens only those with the normal curing schedule (30° C for 24 h) were examined. All fracture surfaces examined were from double cantilever beam specimens.

A Zeiss Ultraphot was used for the optical microscopy using either transmitted or reflected light configurations. The surfaces were cleaned with an ethanol spray to remove loose dust particles in some cases. Scanning electron microscopy was carried out using a Cambridge Stereoscan S4-10 and gold sputter coated specimens.

3. Nomenclature

Previous work on the fractography of polymers has used a confusing variety of terms to describe the fracture surface features. The nomenclature to be used in this work is shown schematically in Fig. 1.

The "arrest line" divides the surface formed during precracking from that formed during reinitiation and growth from the precrack. The "unstable initiation line" separates any slow or subcritical crack growth region from the surface formed by fast, unstable fracture. The surfaces

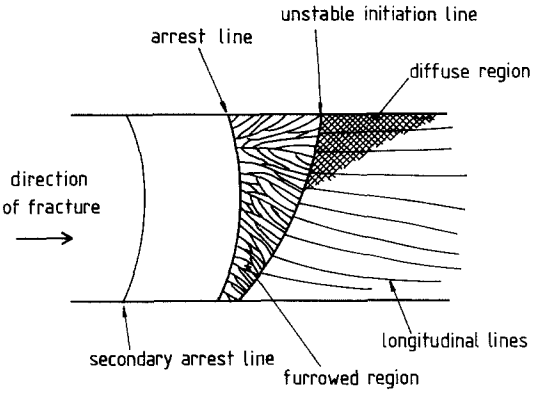

Figure 1 Fracture surface features: definition of terms.

0022–2461/81/071925–10$03.00/0

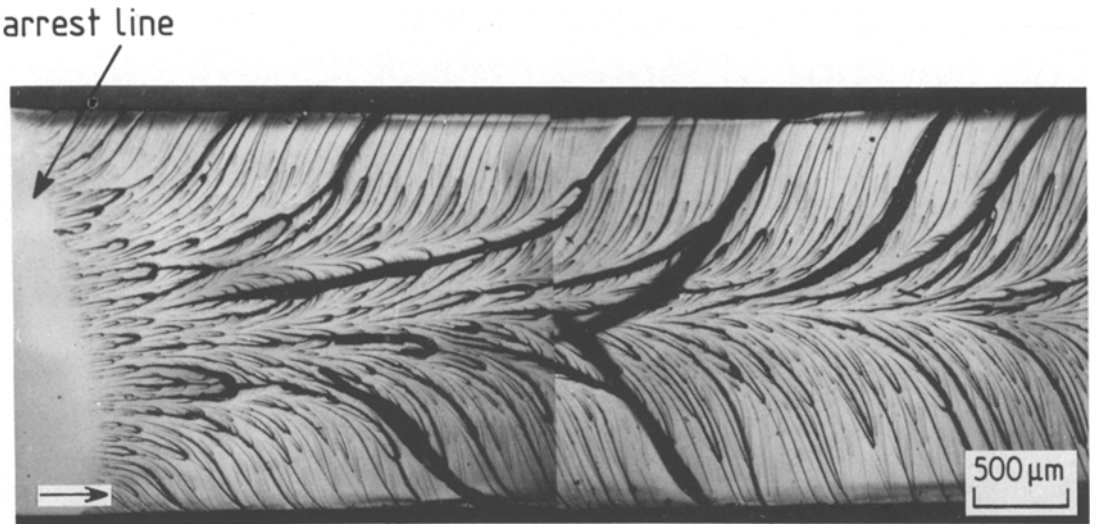

Figure 2 D/TETA: Type IA fracture surface, $\dot{\Delta} = 10^{-3}$ cm min^{-1} (transmitted light).

formed immediately beyond these lines are referred to as the "stable initiation region" and the "unstable initiation region", respectively. These lines may become virtually coincident in some materials, particularly at fast testing rates.

The region between the arrest line and the unstable initiation line is characterized by steps and ridges which become fully developed after about 100 μm of crack growth from the arrest line. This area will be referred to as the "furrowed region".

The principle features of the unstable initiation region are a slightly rough, matte area called the "diffuse region" which has been referred to as "microhackle" or "mist region" by other workers, and a system of fine lines parallel to the crack growth direction called the "longitudinal lines", and described as "fine markings" or "river markings" elsewhere. In some cases the longitudinal lines extend only from restricted areas which appear as depressions or protrusions on the surface. These areas are called "triangular features" [2]. Lines parallel to the crack front but not associated with a true crack arrest are called "secondary arrest lines".

4. Results

The fractography of the two TETA cured systems (D/TETA and 828/TETA) will be reported first since together they display the full range of observed fracture behaviour. Results for the other three systems will then be presented to show that the trends observed for the TETA cured systems are essentially repeated.

4.1. Fractography of D/TETA

4.1.1. Type IA fracture

For fairly slow testing rates (load-point displacement rates up to 0.02 cm min^{-1}), slow stable fracture occurred producing a rough surface with a system of ridges and furrows starting close to the arrest line and diverging away from the centre to meet the specimen edge at about 60° (Fig. 2). There are several prominent lines on the surface which are shown to be sharp steps by scanning electron microscopy (Fig. 3). Occasionally, a fibre-like structure was detached from the surface and appears out of focus in the transmitted light

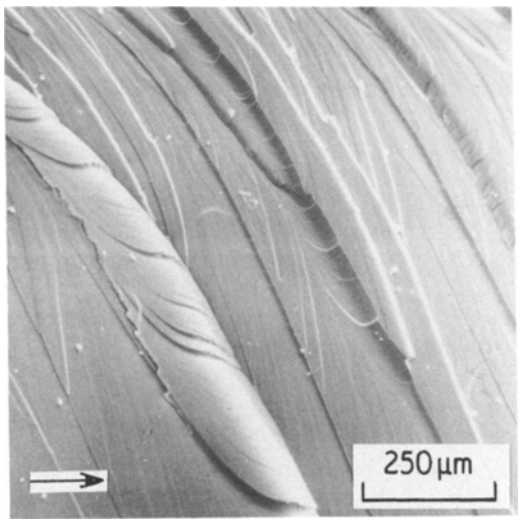

Figure 3 D/TETA: Scanning electron micrograph of steps and ridges in Fig. 2.

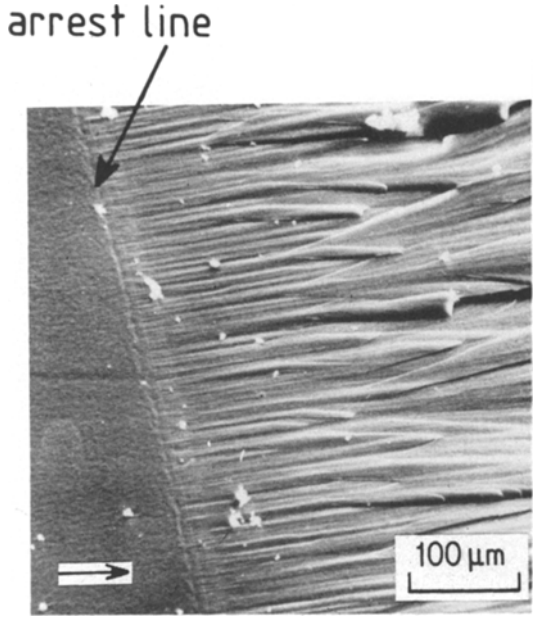

Figure 4 D/TETA: Scanning electron micrograph of initiation region in region in Fig. 2.

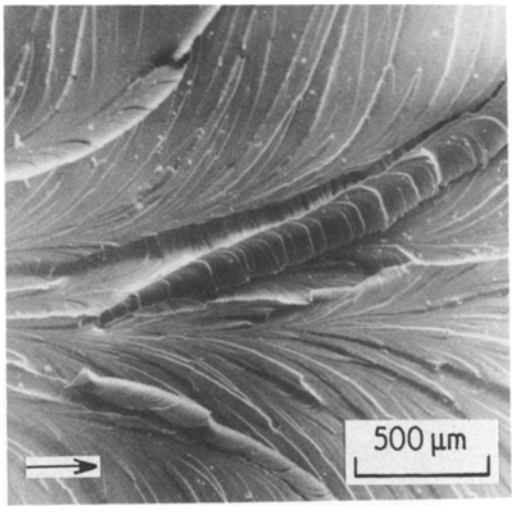

Figure 5 D/TETA: Scanning electron micrograph of fibre formation in Fig. 2.

micrograph (Fig. 2). The steps on the fracture surface appear to be regions of shear fracture connecting adjacent crack fronts on different planes.

At high magnifications, scanning electron microscopy shows a clear arrest line where stable fracture initiated, and a series of fine markings which suggest that there are numerous crack fronts each propagating at a slightly different inclination to the average crack plane (Fig. 4). These merge to form larger flat areas and steps which grow into the ridges and furrows observed further from the arrest line.

Photomicrographs taken with vertical illumination show dark bands extending in to nearly one-third of the specimen thickness from each side. This indicates that the average fracture plane in these bands is oblique to the plane of the central fracture surface, as are the slant fracture bands produced during mixed mode fracture in metals.

The surfaces show no evidence of extensive ductile deformation and are reminiscent of cleavage type fracture. The fibre-like structures detached from the surface appear to be formed by two adjacent steps forming a furrow, followed by cleavage of the fibre from the rut (Fig. 5), rather than by any ductile drawing process. However, a layer of birefringent material below the fracture surface could be observed by viewing through the specimen width with polarized light. Pull-in of the specimen sides was also observed during type IA crack growth and is estimated to be 10 to 20 μm from the change in plane of focus, when observed with a microscope, between the area near the crack and the undisturbed surface. These features, and the observation of slant fracture bands, indicate that extensive anelastic deformation occurred around the crack tip during crack extension and that failure may occur largely in plane stress.

4.1.2. Type IB fracture

At slightly faster testing rates the crack becomes unstable before significant extension has taken place at the specimen sides. The fracture surface has a parabolic shaped furrowed region between the arrest line and the unstable initiation line with identical features to those observed for type IA fracture. In the unstable initiation region the diverging steps and furrows are bent and finer scale markings are produced. These appear to radiate from the tip of the furrowed region where fast fracture must initiate. In cases where a long furrowed region is produced, the markings radiate back along the specimen suggesting that the fast fracture propagated simultaneously forwards and backwards across the remaining intact ligaments along the sides of the specimen (Fig. 6).

At the initiation site of the fast crack there is a smooth mirror zone which is probably associated with very fast crack growth. Beyond this zone the fracture surface has a pattern of fine parabolic

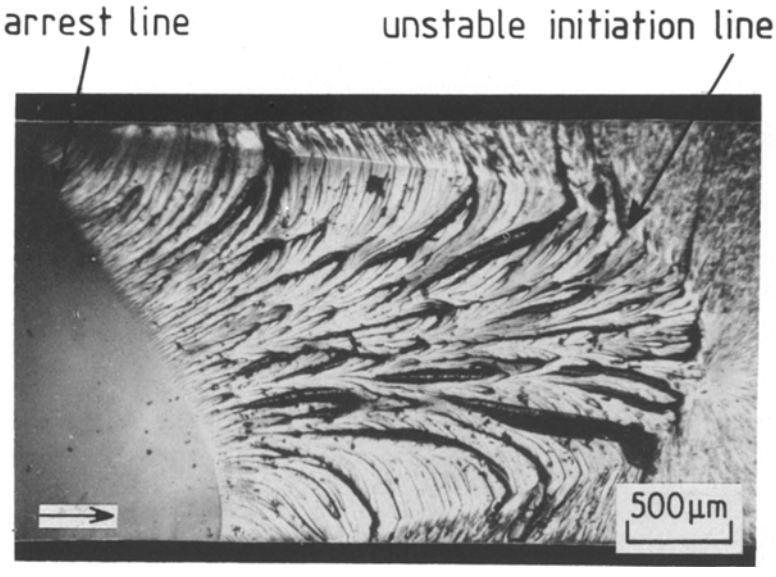

Figure 6 D/TETA: Type IB fracture surface, $\dot{\Delta} = 5 \times 10^{-3}$ cm min^{-1} (transmitted light).

markings. forming a diffuse region, which thin out into a set of longitudinal lines. Eventually, some distance from the unstable initiation line, the surface becomes smooth, glassy and featureless.

4.1.3. Type II fracture

For fast testing rates (load-point displacement rates above 10^{-1} cm min^{-1}) in D/TETA, the load–deflection curve remains essentially linear until fracture, when the crack extends unstably. The rough furrowed region formed at slower testing rates is no longer observed on the fracture surfaces (Fig. 7). The unstable initiation line may still be up to 100 μm from the arrest line which is clearly visible by optical microscopy. The area between the arrest line and the unstable initiation line has fine scale markings very similar to those in the first 50 μm of the stable initiation region for type I fracture. In type I fracture, however, the parallel markings become larger and merged to form the steps and ridges characteristic of slow, stable crack growth. In type II fracture these markings are still small at the unstable initiation line.

Beyond the unstable initiation line, short features extend parallel to the crack propagation direction. Some of these continue along the surface to form longitudinal lines.

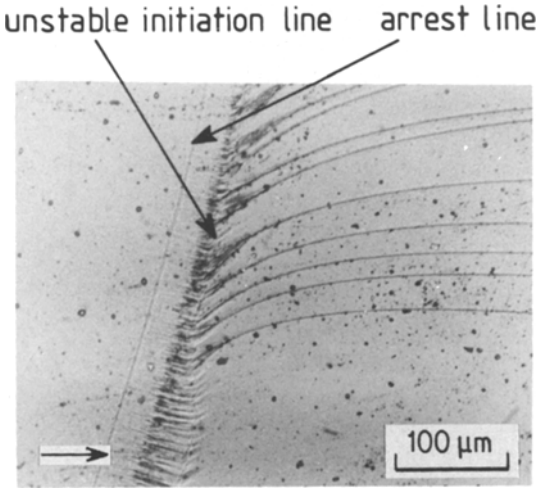

Figure 7 D/TETA: Type II fracture surface, $\dot{\Delta} = 1$ cm min^{-1} (reflected light).

4.2. Fractography of 828/TETA

4.2.1. Type II fracture

Type II fracture persists in this system down to very slow testing rates (5×10^{-4} cm min^{-1}) although more than 100 μm may separate the arrest and unstable initiation lines on the fracture surface. Fine markings parallel to the crack growth direction are again observed in this region (Fig. 8). The unstable initiation line is irregular and the crack appears to have been growing on several different planes when it becomes unstable. These planes are connected by steps in the fracture surface formed beyond the unstable initiation line and result in a system of longitudinal lines. These lines tend to be thicker than those observed on D/TETA fracture surfaces, indicating that the steps are larger. They become finer further from the initiation region and disappear after less than 1 mm to leave a smooth, glassy surface.

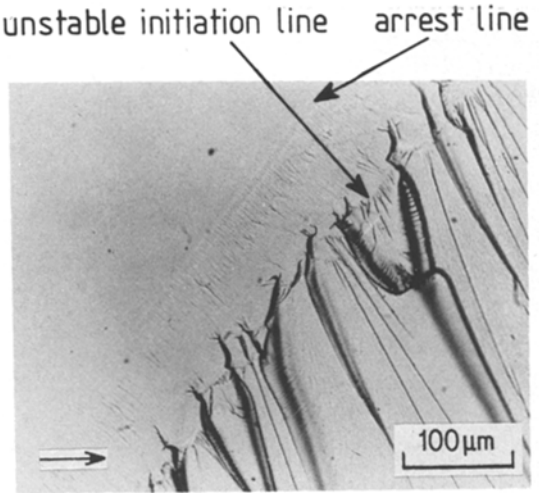

Figure 8 828/TETA: Type II fracture surface, $\dot{\Delta} = 5 \times 10^{-4}$ cm min^{-1} (transmitted light).

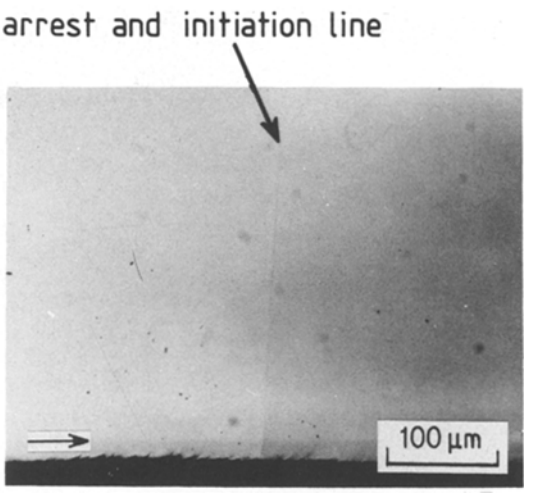

Figure 10 828/TETA: Type III fracture surface, $\dot{\Delta} = 1$ cm min^{-1} (transmited light).

At faster testing rates (5×10^{-3} cm min^{-1}) type II behaviour is still observed but the region between the arrest and unstable initiation lines becomes narrower and the longitudinal lines become shorter, radiating only from localized regions. Fine markings parallel to the crack growth direction can still be resolved in this area. The localized regions where the short longitudinal lines originate appear as depressions or protusions on the surface, starting behind the unstable initiation line and extending up to 100 µm beyond. These triangular features are apparently formed when material is pulled out below the general crack plane as unstable fracture initiates (Fig. 9).

A high density of secondary arrest lines can be observed between arrest lines on the fracture surface.

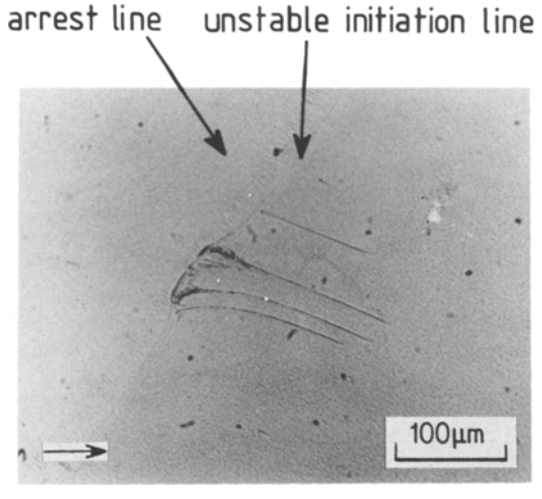

Figure 9 828/TETA: Type II fracture surface, $\dot{\Delta} = 5 \times 10^{-3}$ cm min^{-1} (reflected light).

4.2.2. Type III fracture

As the testing rate is further increased (1 cm min^{-1} or greater), the triangular features disappear and the arrest and unstable initiation lines become coincident (Fig. 10). The load–deflection curve shows a smoothly decreasing characteristic line indicating stable crack growth from the precrack. The fracture surface formed during type III crack growth is smooth and featureless in contrast to the surfaces formed by type I crack growth in D/TETA.

4.3. Fractography of 828/TEPA

In general, the fracture surfaces were very similar to those observed in 828/TETA. At very slow testing rates type II behaviour occurred and the arrest and the unstable initiation lines were less than 10 µm apart. No fine markings parallel to the crack growth direction could be resolved. Longitudinal lines are observed (Fig. 11) but extend more than 1 mm only for very slow testing rates (0.001 cm min^{-1}). At faster testing rates these features extend less than 100 µm from the unstable initiation line. No diffuse region was observed but secondary arrest lines are common and appear to be formed by sudden excursions of the crack front out of the average fracture plane.

The arrest and initiation lines are coincident and very thin after stable type III fracture. The fracture surface is completely smooth and glassy

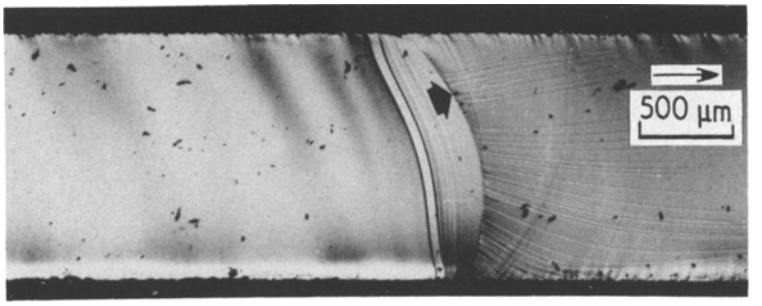

Figure 11 828/TEPA: Type II fracture surface, $\dot{\Delta} = 10^{-3}$ cm min^{-1} (transmitted light).

with no longitudinal lines or other features extending from the initiation line.

4.4. Fractography of D/TEA

At very slow testing rates (0.001 cm min^{-1}) the fracture surface (Fig. 12) showed a furrowed region between the arrest line and unstable initiation line with features very similar to those observed for D/TETA type I fracture surfaces. This furrowed region corresponds to the stable crack extension. It extends up to 1 mm along the surface with a pattern of markings generally parallel to the crack growth direction which tend to merge to form larger steps towards the unstable initiation line. Comparison with D/TETA fracture surfaces shows that the D/TEA surface has finer scale features. The large steps, ridges and detached fibres observed for D/TETA are not observed. There is no evidence of extensive slant fracture or side pull-in.

The steps in the furrowed region continue across the unstable initiation line with a change in direction. Further from the initiation line the ridges become smaller and less sharp. They form a diffuse region extending up to 2 mm down the surface, finally leaving a set of longitudinal lines on a smooth glassy surface.

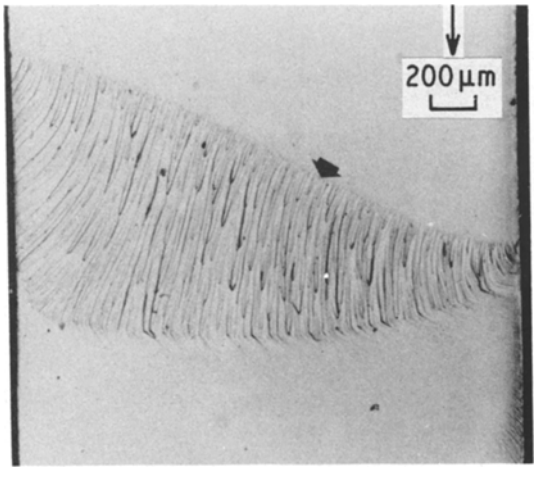

Figure 12 D/TEA: Type IB fracture surface, $\dot{\Delta} = 10^{-3}$ cm min^{-1} (transmitted light).

When the testing rate was increased the furrowed region decreased in length to about 100 μm at 5 cm min^{-1}, but the surface features remained essentially similar to those formed at slower testing rates. The diffuse region and longitudinal lines in the region beyond the unstable initiation line also became shorter, extending only about 50 μm at 5 cm min^{-1} load-point displacement rate.

4.5. Fractography of 828/TEA

Unstable type II fracture was observed for this system over the entire range of testing rates used (0.002 to 10 cm min^{-1}). Some variation in fracture surface features was found which correlated with the testing rate.

At slow testing rates, a region up to 100 μm long was observed between the arrest and unstable initiation lines which again shows features similar to the slow stable fracture surfaces in D/TETA. Fine markings are visible parallel to the crack growth direction which merge to form larger steps as the crack extends (Fig. 13). Unstable fracture appears to initiate first in one region of the unstable initiation line towards the centre of the fracture plane and markings on the subsequent fracture surface radiate from this point. A very long diffuse area extends more than 8 mm along the surface (Fig. 14). It consists of a dense system of fine ridges on the surface spaced about 5 μm apart and becoming highly regular and parallel beyond the immediate initiation region.

Of particular interest are detached fibres 1 or 2 μm in diameter which are visible over a wide area of the diffuse region. Microscopy suggests that the fibres have irregular surfaces and appear to be formed by brittle cleavage from the ridges on the

Figure 13 828/TEA: Type II fracture surface, $\dot{\Delta} = 5 \times 10^{-3}$ cm min^{-1} (transmitted light).

fracture surface (Fig. 14). In some cases they become reattached further along the surface.

At faster testing rates (0.1 cm min^{-1} or faster) complex arrest and initiation regions are observed consisting of several interconnecting lines across the specimen width. They must be formed during

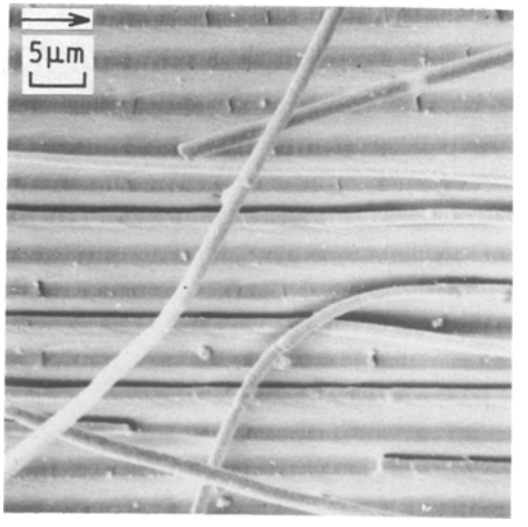

Figure 14 828/TEA: Scanning electron micrograph of diffuse region in Fig. 13.

initiation rather than during deceleration of the precrack since they are not visible on fracture surfaces tested at slow rates. The initiation lines are well defined but there are no furrowed regions. A diffuse region similar to that formed in slow tests was visible and decreased in length with increasing testing rate. The ridges were less regular and no detached fibres were observed.

5. Discussion

5.1. Fracture surface features

The fracture surface features which are observed at various testing rates are summarized in Fig. 15. This may be compared with the summary of fracture behaviour in the previous paper ([1] Fig. 13).

The furrowed region can be correlated with slow stable crack growth and type I loading curves for D/TETA and D/TEA at slow testing rates. However, similar features are also observed for slow testing rates with 828/TETA and 828/TEPA when type II behaviour is obtained. It is therefore highly probable that these furrowed regions were also formed by slow stable growth preceding fast unstable type II propagation. This does not conflict with the shape of loading curve (which showed no increase in compliance during loading) since the compliance change for the length of crack extension involved is not detectable. Very similar furrowed zones have been reported in polyester resins [3]. They were observed to increase in length with the addition of a flexibilizer. Furrowed zones have also been observed previously in other epoxy

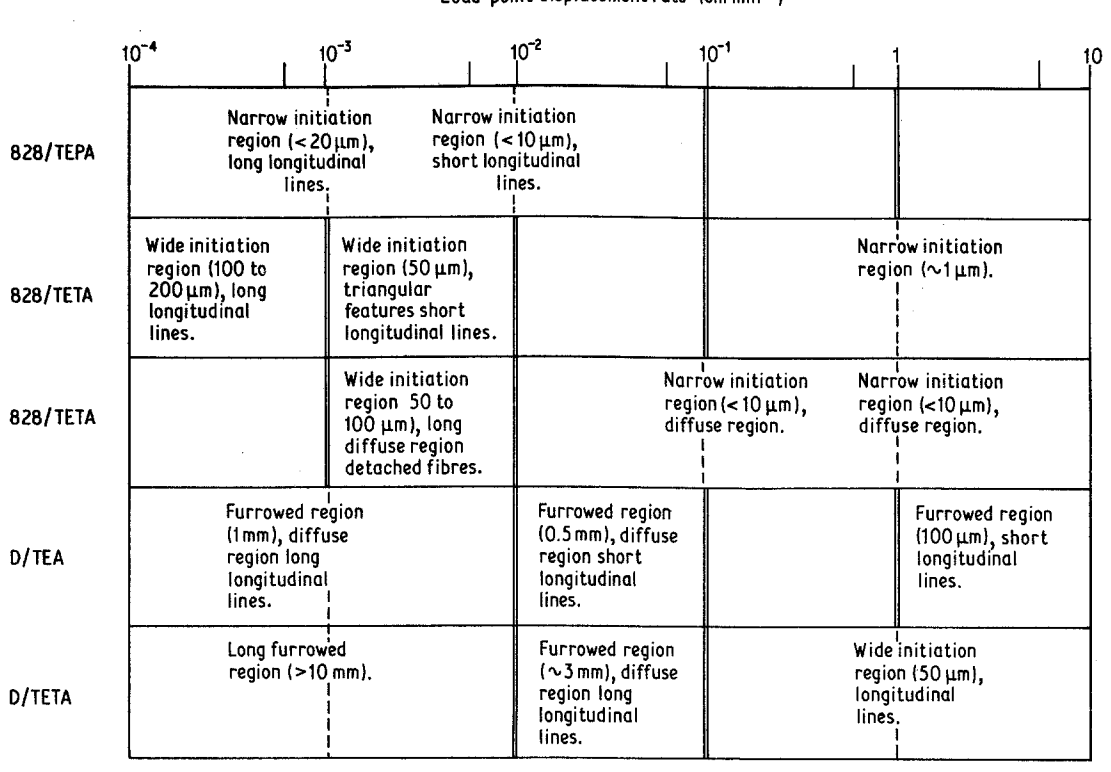

Figure 15 Summary of fracture surface features.

resin systems [2, 4] and have been associated with slow crack growth [5, 6].

The origin of the fracture surface steps is not clear but they may be associated with the large plastic zone and large crack opening displacement which probably exists during type I propagation. There is evidence from slant fracture bands, pull-in of the specimen sides and residual birefringence through the specimen thickness after type IA fracture, that extensive plastic deformation occurs during crack growth. Plane stress conditions are probably approached for D/TETA at low testing rates since the plane stress plastic zone size, r_y, may be calculated to be about 0.5 mm using the following equation [7],

$$r_y = \frac{EG}{2\pi\sigma_y^2} \quad (1)$$

with $E = 2.9\,\text{GPa}$, $\sigma_y = 54\,\text{MPa}$ and $G = 3\,\text{kJ m}^{-2}$ for type I crack growth in D/TETA. The through thickness stress should relax over this distance inwards from each side. This corresponds to the slant fracture band width visible with reflected light on the type IA surface. These slant fracture bands are not at 45° as in metals and appear to be formed by the relaxation of the plane stress region after the crack has extended through the fracture plane.

Triangular features have previously been observed [2] in 828/TETA systems and it was suggested that they are associated with undercuring. These features were not, however, observed in the other undercured systems examined here. Diffuse regions have been commonly observed [5, 8] in the unstable growth region and have been found to become longer at higher testing temperatures [2]. This would be expected from the results presented here which show that the diffuse region increases in length as testing rate is decreased. Long diffuse regions with parallel ridges and detached fibres very similar to those observed on 828/TEA fracture surfaces have been observed previously with phenol–formaldehyde [9, 10] and polyester [8] resins. Nelson and Turner [11] proposed a mechanism for the formation of the fibres by the curling of ribbons of detached surface film. The results presented here suggest that they are formed by a brittle cleavage process.

5.2. Fracture behaviour

Recently, Yamini and Young [6] suggested that the furrowed region is due to the extension of the

crack through a Dugdale type plastic zone. They examined the furrowed zones on epoxy fracture surfaces and found some agreement between the length of the furrowed zone and the length of the plastic zone calculated using the measured fracture toughness and yield stress in the Dugdale [12] model. Although this may be reasonable over a restricted range of testing rates it obviously does not fully describe the type I behaviour observed here. The correlation with minimum post-yield stress shown previously [1] suggests that fracture behaviour may be explicable in terms of the dependence of yield stress on strain rate.

The strain rate experienced by material at the end of the yielded zone and in the fracture plane may be described by the Irwin [13] relation,

$$\dot{\epsilon} = \frac{\dot{\sigma}}{E} \simeq \frac{\sigma_y}{E} \frac{\dot{K}}{K} + \frac{\dot{a}}{2r_y} \quad (2)$$

where σ_y is the appropriate yield stress, E is the elastic modulus, K is the stress intensity factor, and $\dot{K}$ is its derivative with respect to time, $\dot{a}$ is the crack velocity and r_y is the radius of the yielded zone. The derivation of this equation assumes a constant yield stress and modulus but should be adequate for the present, essentially qualitative model.

For a stationary crack the second term in Equation 2 will be zero and $\dot{K}/K$ may be approximated by $2/t$ where t is the time elapsed since the start of monotonic loading [13]. Hence,

$$\dot{\epsilon} \simeq \frac{\sigma_y}{E} \frac{2}{t} \quad (3)$$

and the strain rate at the end of the yielded zone will be small provided t is large.

When some critical condition (such as a critical crack opening displacement) is reached, the crack will begin to propagate. The strain rate will then be described by Equation 2. The first term must decrease as the crack propagates in a displacement controlled test because the specimen compliance increases. $\dot{a}$ is greater than zero; however, since r_y may also increase as the toughness increases the second term on the right-hand side of Equation 2 may still be small. Hence the strain rate at the tip of the yielded zone will not necessarily increase provided that the crack velocity is small. Thus the yield stress may remain low and the crack can continue to grow slowly and stably.

An increase in testing rate may, however, cause the second term to become larger and increase the effective strain rate at the tip of the yielded zone. This increase in strain rate will result in an increase in the yield stress and since this leads to a decrease in the size of the yielded zone the strain rate will rise rapidly, causing a sudden transition to a more brittle type of crack growth with a much smaller yielded zone and fracture surface energy. The crack will thus become unstable.

The transition from slow stable to fast unstable fracture cannot be explained on the basis of a plane stress to plane strain transition because limited slow stable growth has been inferred to occur under plane strain conditions from fractographic evidence from the high yield stress resins.

For fast stable fracture to occur, the initiation toughness must be comparable to the propagation toughness. As the testing rate is further increased in Equation 3, the first term will increase so that the effective strain rate is high during loading to crack initiation. The yield stress will also be high and the yielded zone will be small. Provided the yielded zone developed during loading is comparable in size to the yielded zone ahead of the propagating crack, fast stable fracture may take place.

6. Conclusions

Slow, stable or subcritical crack extension is associated with the formation of a furrowed fracture surface. This type of behaviour is promoted by slow testing rates and the presence of a plasticizer in the resin. Comparison with other work suggests that this may be a common mode of fracture in epoxy resins, including fully cured systems, and possibly in highly crosslinked polymers in general.

The length of the stable growth region decreases as the testing rate is increased, but disappears only when fast, stable crack growth occurs.

The mechanism of fracture does not appear to involve void growth or fibrillation. There was, however, evidence of fairly extensive plastic deformation in a layer below the fracture surface in the plasticized epoxy.

The transitions in fracture behaviour have been qualitatively explained in terms of the effect of strain rate on yielding.

References

1. B. W. CHERRY and K. W. THOMSON, *J. Mater. Sci.* **16** (1981) 1913.
2. S. YAMINI and R. J. YOUNG, *ibid.* **14** (1979) 1609.
3. M. J. OWEN and R. G. ROSE, *J. Phys. D. App. Phys.* **6** (1973) 42.

4. J. MIJOVIĊ and J. A. KOUTSKY, *Polymer* **20** (1979) 1095.
5. D. C. PHILLIPS, J. M. SCOTT and M. JONES, *J. Mater. Sci.* **13** (1978) 311.
6. S. YAMINI and R. J. YOUNG, *ibid.* **13** (1980) 1823.
7. J. F. KNOTT, "Fundaments of Fracture Mechanics", (Butterworths, London, 1973).
8. A. CHRISTIANSEN and J. B. SHORTALL, *J. Mater. Sci.* **11** (1976) 1113.
9. B. E. NELSON and D. T. TURNER, *J. Polymer Sci. A2* **10** (1972) 2461.
10. R. A. SPURR, E. H. ERATH, H. MYERS and D. C. PEASE, *Ind. Eng. Chem.* **49** (1957) 1839.
11. B. E. NELSON and D. T. TURNER, *J. Polymer Sci. 13* **9** (1971) 677.
12. D. S. DUGDALE, *J. Mech. Phys. Sol.* **8** (1960) 100.
13. G. R. IRWIN, *Appl. Mater, Res.* **3** (1964) 65.

Received 28 February 1980 and accepted 7 January 1981.